SAND2020-3615C

Dynamic Coverage Control and Stochastic Multi-Target Tracking with Multiple Pursuers

Milad Khaledyan, Kendric Ortiz, Meeko Oishi, and John Richards

***Abstract*— We address the problem of simultaneous coverage control and stochastic, multi-target tracking with multiple pursuers with limited range sensors. We formulate the problem as a constrained stochastic optimization problem that is non-convex due to the joint sensing model. We exploit the closed-form solution of the forward stochastic reach set to estimate the joint likelihood of target locations, and construct an open-loop control policy for the pursuers. We numerically evaluate our approach in simulation experiments, and show that computational complexity is dependent of the number of pursuers, but not on the number of targets. Our results indicate that this approach can be used to construct optimal mobile sensor trajectories, in accommodate complex, stochastic environments with realistic sensing models.**

I. Introduction

We consider the problem of UAV-based simultaneous tracking and coverage in stochastic, dynamic environments, which is necessary for data collection, remote observation, search and rescue, and other applications. In many cases, UAVs are deployed as mobile sensors to monitor dynamic and uncertain phenomena. Positioning of the UAVs depends not only upon the location of relevant phenomena on the ground, but also on the UAV's sensing capabilities, and may be subject to a variety of other constraints (i.e., fuel minimization, flight time constraints, collision avoidance). Further, coordination amongst UAVs in fleets is needed leverage sensing from individual UAVs, to minimize duplication due to sensor overlap.

Much of work in coverage and tracking applications has focused on coordination amongst vehicles via distributed control, in an environment which is presumed to be deterministic, although potentially time-varying. Gradient-based controllers allow the vehicles to optimally navigate through a region of interest while exploiting sensing performance [1]–[4]. However, a similar foundation in stochastic environments is lacking. *Our focus is on problem of simultaneous coverage and tracking in stochastic dynamic environments, with multiple vehicles that have sensing limitations.*

One approach to this problem employs a partitioning of the environment, so that each pursuer is responsible for one cell in the partition. In [5], [6] the authors presume that the position of the target is discontinuous, and modeled by a random variable. These methods translate the stochastic behavior of the targets in the density function directly, and utilize a time-varying probability density function to account for both target tracking and coverage tasks. In [7], the authors use decentralized adaptive control to drive a network of mobile robots in the direction of an optimal sensing configuration [7]. The time-varying density function is unknown, and the robots acquire this information online using an adaption law from sensory measurements.

Information theoretic methods seek to simultaneously achieve stochastic coverage and exploration. A mutual information approach that utilizes a particle filter representation has been used in [8] to design a scalable method that localizes a stationary target and explores an unknown region using multiple robots. In [9], the authors suggest an exploration via optimal SLAM control that exploits the gradient of mutual information; the targets' states are assumed to be discrete random variables which are estimated by a linear consensus algorithm. In [10], the authors propose a filter to estimate the targets' joint density, instead of estimating individual target locations. This approach maximizes the acquired information regardless of number of targets. An ergodic receding horizon approach was proposed in [11], that avoids exhaustive search and uses sensor feedback to adaptively update the expected information density [12].

Some work has also been done to exploit the joint detection by all sensors. The authors in [13], [14] consider limited-range sensors, and employ a joint probability detection function A consensus-based method was investigated in [15], that maximizes the probability of consensus target detection among mobile sensors, but with significant computational complexity. Other work has employed both sensor-consensus and sensor-fusion for sensor deployment problems [16].

Our approach invokes an optimization framework inspired by [1], but that can handle stochastic target dynamics as well as the shared observation by multiple pursuers, which have limited range sensors. We employ results from forward stochastic reachability analysis [17] to determine the

This material is based upon work supported in part by the National Science Foundation under Grant Number IIS-1528047. Any opinions, findings, and conclusions or recommendations expressed in this material are those of the authors and do not necessarily reflect the views of the National Science Foundation. This research was also supported in part by the Laboratory Directed Research and Development program at Sandia National Laboratories, a multimission laboratory managed and operated by National Technology and Engineering Solutions of Sandia, LLC., a wholly owned subsidiary of Honeywell International, Inc., for the U.S. Department of Energy's National Nuclear Security Administration under contract DE-NA-0003525. The views expressed in this article do not necessarily represent the views of the U.S. Department of Energy or the United States Government. This research was also supported in part by the University of New Mexico, Vice President for Research Office, through LDRD/ACORN Supplemental Funding.

M. Khaledyan is with Path Robotics, Inc, Dayton, OH. His work on this was completed while he was a Postdoctoral Associate at the University of New Mexico.

K. Ortiz and M. Oishi are with the Department of Electrical and Computer Engineering, University of New Mexico, Albuquerque, NM. Corresponding author: oishi@unm.edu

J. Richards is with Sandia National Laboratories, Albuquerque, NM.

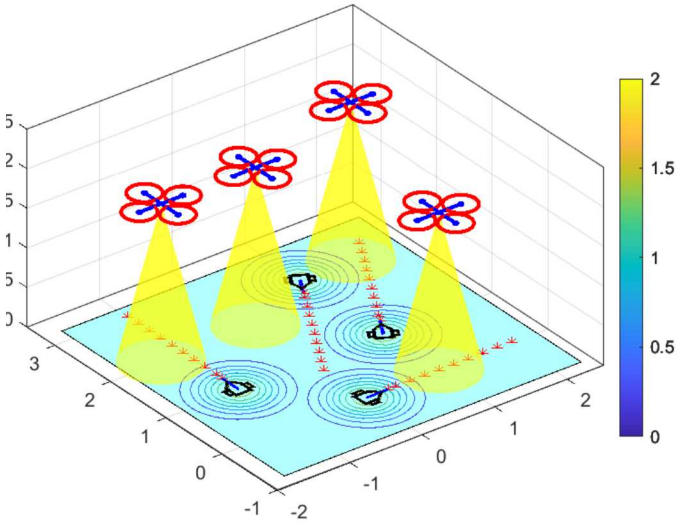

Fig. 1. Aerial vehicles (the pursuers) must assure coverage of the environment as well as tracking of stochastic ground vehicles (the targets). The mean trajectories for the targets are depicted by '*', and level sets of each targets' initial probability density functions are also shown.

likelihood of the targets' position, as well as the forward reachable set of the pursuer to ensure that pursuers can coordinate to reach the desired locations at the desired time. The main advantage of our framework is that it its computational complexity is independent of the number of targets we wish to observe, and that it accommodates the potential for joint detection amongst multiple sensors. In lieu of artificially partitioning the environment, collision avoidance constraints are embedded within the optimization. While non-convex, first and second derivatives are available to facilitate nonlinear methods such as sequential quadratic programming.

The remainder of the paper is as follows: Mathematical preliminaries and the problem formulation are given in Section II. We characterize optimization problems for pursuer trajectories and for the corresponding optimal control in Section III. Section IV provides numerical results from simulation. A summary is presented in Section V.

II. Problem Setup

We consider the problem of simultaneous optimization of coverage and tracking of multiple stochastically moving targets by multiple pursuers in a bounded and predefined environment of interest $Q \subset \mathbb{R}^m$, as in Fig. 1.

A. Target and pursuer dynamics

We model the i^{th} target as a linear time-invariant dynamical system

$$x^i_{t+1} \quad = \quad Ax^i_t + B\omega^i_t, \tag{1}$$

with state $x^i \in \mathbb{R}^m$, disturbance process $\omega^i \in \mathcal{W} \subseteq \mathbb{R}^p$, and constant matrices A, B, of appropriate dimensions, for $i \in \{1, \cdots, N\}$. We presume w^i is an independent and identically distributed random vector in the probability space $(\mathcal{W}, \sigma(\mathcal{W}), \mathbb{P}_\omega)$ defined by sample space $\mathcal{W}$, sigma-algebra $\sigma(\mathcal{W})$, and probability measure $\mathbb{P}_\omega(\omega \in \mathcal{B}) = \int_{\mathcal{B}} \psi_\omega(q)dq$ for probability density function $\psi_\omega : \mathbb{R}^p \to \mathbb{R}$ and a Borel set $\mathcal{B} \in \sigma(\mathcal{W})$ [18].

We define the likelihood that the i^{th} target is at a location $q \in Q$ at time t as $\phi^i_t(q) : \mathbb{R} \to [0, 1]$. Let $\mathcal{E}^i_t$ be the event that the i^{th} target is located within the interval $[q, q + dq]$ at time t, then we have

$$\mathbb{P}(\mathcal{E}^i_t) = \phi^i_t(q)dq. \tag{2}$$

We define the *aggregate* relative likelihood that there exists a target within the desired interval, that is,

$$\Phi_t(q) = \mathbb{P}\left(\bigcup_{i=1}^{n} \mathcal{E}^i_t\right). \tag{3}$$

We also model the i^{th} pursuer as a linear time-invariant dynamical system

$$p^i_{t+1} = A_{\text{Pursuer}}p^i_t + B_{\text{Pursuer}}u^i_t \tag{4}$$

with state $p^i \in \mathcal{X} \in \mathbb{R}^m$, controlled input $u^i \in \mathcal{U} \subseteq \mathbb{R}^r$, and system matrices A_{Pursuer}, B_{Pursuer} of appropriate dimensions for $i \in \{1, \cdots, n\}$. Let $u^i_t = \pi^i_t$ be an open-loop control action, and $\mathcal{M}$ be the set of all feasible control policies. We define the one-step reach set for the i^{th} pursuer at time t,

$$\text{Reach}(p^i_t) = \{\bar{y} \in \mathcal{X} \mid \exists \pi^i_t \in \mathcal{M} \text{ s.t. } p^i_t = \bar{y}\} \tag{5}$$

with open-loop control sequence $\pi^i_t = \{u^i_0, u^i_1, \ldots, u^i_{t-1}\}$ [17].

B. Pursuer sensing model

We presume each pursuer is equipped with a range sensor, and that signal strength decays with the Euclidean distance between the sensor and the source. We describe exponentially decaying sensing performance for the i^{th} pursuer in terms of the sensing function $f^i : \mathbb{R}_{\geq 0} \to [0, 1]$,

$$f^i(\|q - p^i\|) = f^{i0}e^{-\lambda_i \|q-p^i\|^2} \tag{6}$$

in which $\lambda_i \in \mathbb{R}_+$ and $f_{i0} \in (0, 1]$ depend on the physical characteristics of the sensor. For $\mathcal{A}^i_t$ that denotes the event in which the i^{th} pursuer located at p^i detects the source at $q \in Q$ at time t, we have that $\mathbb{P}(\mathcal{A}^i_t) = f^i(\|q - p^i\|)$. That is, the sensing function describes the likelihood of the i^{th} sensor detecting a target at location q.

Because sensing regions associated with multiple pursuers can overlap, we must account for the likelihood of joint detection by multiple pursuers. We represent the event that there exists at least one pursuer that detects a target at location $q \in Q$ at time t as $\cup^n_{i=1}\mathcal{A}^i_t$, hence the joint probability of detection is $\mathbb{P}(\cup^n_{i=1}\mathcal{A}^i_t)$. Assuming that pursuer observations are obtained independently, i.e., $\mathbb{P}(\mathcal{A}^i_t \cap \mathcal{A}^j_t) = \mathbb{P}(\mathcal{A}^i_t) \cdot \mathbb{P}(\mathcal{A}^j_t)$, we apply the inclusion-exclusion principle to obtain

$$\mathbb{P}\left(\bigcup_{i=1}^{n} \mathcal{A}^i_t\right) = 1 - \prod_{i=1}^{n}\left[1 - \mathbb{P}(\mathcal{A}^i_t)\right] \tag{7}$$

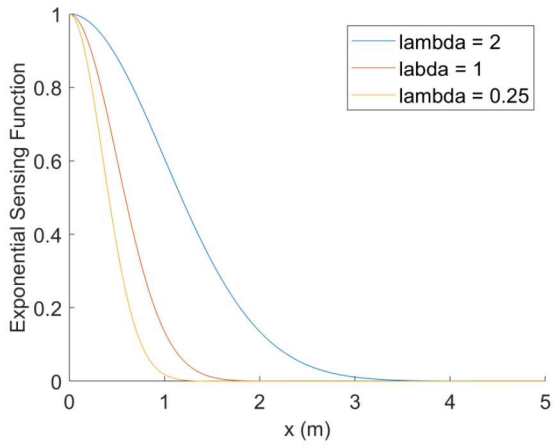

Fig. 2. Sensing function (6), for $\lambda_i = 0.25$, $\lambda_i = 1$, and $\lambda_i = 2$, with $f^{i0} = 1$. For a norm-based distance x, the sensing function describes the ability of the sensor to accurately evaluate information a distance x from the sensor.

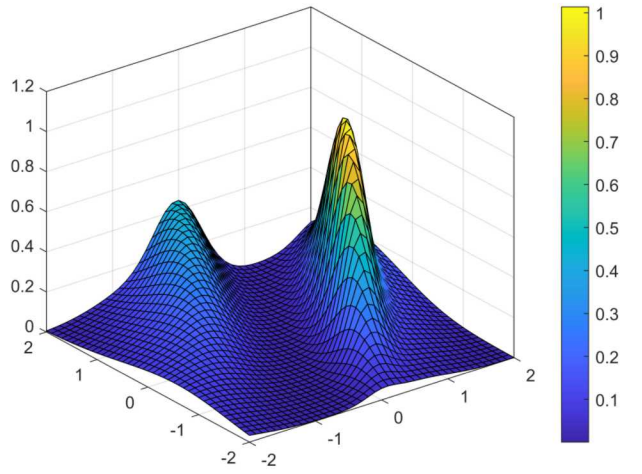

Fig. 3. Aggregate density overapproximation, $\bar{\Phi}(q_t)$, generated from a sum of four individual density functions, $\phi^i(q_t)$, each of which is described by a Gaussian distribution $\mathcal{N}(\mu, \sigma)$ for $\mu = xx$ and $\sigma = yy$.

Denoting $\mathcal{F}(q, p_t) = \mathbb{P}(\cup_{i=1}^n \mathcal{A}_t^i)$, and applying (6), we rewrite (7) to obtain the joint probability of detection by all pursuers

$$\mathcal{F}(q, p_t) = 1 - \prod_{i=1}^{n} \left[1 - f^i(\|q - p_t^i\|)\right]. \tag{8}$$

As opposed to the case in which there is a single pursuer [19], (8) is important because it accounts for the potential for simultaneous observation by multiple sensors. Without accounting for the joint probability of detection, pursuers could select trajectories which essentially duplicate work being done by other pursuers.

III. Optimal Pursuer Trajectories and Control

We seek to maximize the likelihood that with a given set of pursuers, we can optimally cover a bounded region and track anticipated target movement. To do so, we separate the problems of trajectory optimization and controller synthesis into two problems, solved sequentially. Feasibility of resulting trajectories is ensured by capturing pursuer dynamics in the trajectory optimization problem.

A. Optimization of Pursuer Trajectories

We draw upon an approach originally described in [3], in which coverage and tracking over a pursuer-partitioned space is accomplished through maximization of an *expected-value multi-center function*, that captures limitations of sensing performance, weighted by the relative importance of the area to the covered.

Definition 1 (Expected-value multi-center function [3]) *From Ch. 2.3.1 in [3]. Given a bounded measurable set $Q \subseteq \mathbb{R}^m$, points $p_i \in \mathbb{R}^m$, $i \in \{1, \ldots, n\}$, an importance function $\psi : \mathbb{R} \to \mathbb{R}_{\geq 0}$, and a performance function $f : \mathbb{R}_{\geq 0} \to \mathbb{R}$, that is non-increasing and piecewise continuously differentiable, the function $H : \mathbb{R}^m \to \mathbb{R}$, such that*

$$H(p_1, \cdots, p_n) = \int_Q \max_{i \in \{1, \cdots, n\}} f(\|q - p_i\|)\psi(q)dq \tag{9}$$

is an expected-value multi-center function.

Solving (9) results in a choice of p_i that optimally cover a region S, weighted by the importance function ψ, for some sensing performance f that is uniform for all points p_i. While it is straightforward to employ the aggregate relative likelihood (3) as the importance function, the fact that we employ a non-partitioned approach to pursuer positioning means that replacing the performance function with individual pursuer sensing functions (6) will be ineffective. Instead, we re-interpret the maximization over all sensing functions to accommodate the potential for joint sensing.

$$\mathcal{H}(p_t^1, p_t^2, \ldots, p_t^n) = \int_Q \mathcal{F}(q, p_t)\Phi_t(q)dq \tag{10}$$

However, the aggregate likelihood $\Phi_t(\cdot)$ is in general difficult to compute. By Boole's inequality, the upper bound

$$\Phi_t(q) \leq \sum_{i=1}^{n} \mathbb{P}(\mathcal{E}_t^i) \tag{11}$$

is straightforward to compute, since

$$\sum_{i=1}^{n} \mathbb{P}(\mathcal{E}_t^i) = \sum_{i=1}^{n} \phi_t^i(q) \triangleq \overline{\Phi}_t(q). \tag{12}$$

Hence we obtain the approximation

$$\overline{\mathcal{H}}(p_t^1, p_t^2, \ldots, p_t^n) = \int_Q \mathcal{F}(q, p_t)\bar{\Phi}_t(q)dq \tag{13}$$

that represents the objective function we wish to maximize through pursuer trajectory selection. Fig. 3 depicts the overapproximation $\bar{\Phi}_t(q)$ for a scenario in which each of four targets generates a Gaussian likelihood $\phi_t^i(q)$.

We maximize (13) to optimize the joint probability of detection, weighted by an overapproximation of the likely

target positions. Hence we seek to solve following optimization problem:

$$\begin{aligned} \underset{p_t^1, p_t^2, \ldots, p_t^n}{\text{maximize}} \quad & \sum_{t=1}^{T} \mathcal{H}(p_t^1, p_t^2, \ldots, p_t^n) \\ \text{subject to} \quad & p_t^i \in \text{Reach}(p_{t-1}^i),\ \forall i \in \{1, \ldots, n\} \\ & r_{\min} - \|p_t^i - p_t^j\| \leq 0,\ \forall j \in \{1, \ldots, n : j \neq i\} \end{aligned} \tag{P1}$$

The decision variables are the positions of the pursuers, $p_t = (p_t^1, p_t^2, \ldots, p_t^n)$, over a time horizon of length T. The pursuer positions are subject to pursuer dynamics under open-loop control, via the one-step reachable set (5), in the first constraint. The second constraint assures collision avoidance.

B. Numerical computation

First, we note that the constraint associated with the dynamics of the pursuer are convex.

Lemma 1 *[20, Section 5] If the control space $\mathcal{U}$ is convex, the reach set* $\text{Reach}(p_t)$ *is convex.*

Computation of the one-step reach set is straightforward via MPT [21].

Second, we note that the forward stochastic reach probability density [17] provides a closed-form expression for $\bar{\Phi}(q_t)$ in (12), the over-approximation of the aggregate relative likelihood.

Lemma 2 *[17, Proposition 1] For all $i = 1, \ldots, N$, and $t \in [1, T]$, Let $x_0^i \in \mathcal{X}$ be the known initial position for the i^{th} target in (1), and random process $\omega^i \sim \mathcal{N}(\mu_{\omega^i}, \Sigma_{\omega^i}) \in \mathbb{R}^p$, then the system trajectory of (1) is*

$$\phi_t^i(\cdot) \sim \mathcal{N}(\mu_t^i, \Sigma_t^i) \tag{14}$$

where

$$\mu_t^i = A^t x_0^i + \mathcal{C}_t(\mathbf{1}_{t\times 1} \otimes \mu_{\omega^i}) \tag{15}$$

$$\Sigma_t^i = \mathcal{C}_t(I_t \otimes \Sigma_{\omega^i})\mathcal{C}_t^\intercal \tag{16}$$

$\mathcal{C}_t = [B \;\; AB \;\; A^2B \;\; \ldots \;\; A^{t-1}B] \in \mathbb{R}^{n\times(tp)}$ is the controllability matrix for system (1), and I_t is the $t\times t$ identity matrix.

Lemma 2 provides closed-form expressions for each target separately; (12) is constructed from their sum.

Lastly, there are non-convexities associated with both the collision avoidance constraint as well as the objective function in (P1).

Unfortunately, unlike in the single-pursuer case [19], which exploits concavity of the sensing function f and non-negativity of the density function $\bar{\Phi}_t(q)$ to assure convexity of the objective function [1, Lemma 3.8], the objective function (13) is non-convex. While $\bar{\Phi}_t(q)$ clearly satisfies the non-negativity property, the joint sensing function (8) is not concave. However, solutions to (P1) are amenable to gradient-based methods, since analytical expressions are available for first and second derivatives of (13).

By taking partial derivative of (13) with respect to the i^{th} pursuer's location p_t^i at time t, we obtain

$$\begin{aligned} \frac{\partial \mathcal{H}}{\partial p_t^i} &= \int_Q \frac{\partial \mathcal{F}(q, p_t)}{\partial p_t^i} \bar{\Phi}(q) dq \\ &= \int_Q \left[\frac{p_t^i - q}{\|q - p_t^i\|} \frac{\partial f^i}{\partial \|q - p_t^i\|} \prod_{k=1, k\neq i}^{n} (1 - f^k) \right] \bar{\Phi}_t(q) dq \end{aligned} \tag{17}$$

The analytical expression for the Hessian matrix of the objective function can be similarly obtained, but is omitted here due to space limitations.

Since the closed-form expression for the gradient and Hessian matrix of the objective function are available, and the objective function and the constraints are continuous and have continuous first derivatives, we can employ numerical solutions based in sequential quadratic programming [22, Chapter 18], interior point methods [23], or difference-of-convex programming [24] for locally optimal solutions.

We also note that the choice of time horizon will have a significant impact on the computation time in solving (P1). While moderately longer time horizons may improve capacity to plan, shorter time horizons can improve compute time and responsivity to current information [25].

C. Controller synthesis

Presuming a solution to (P1) has been obtained, we then pose an optimization problem construct the control law for each pursuer. Let $u_t = (u_t^1, u_t^2, \ldots, u_t^n)$ be the concatenated vector of all pursuers' controls. We design an open-loop control policy via the following optimization problem,

$$\begin{aligned} \underset{u_t}{\text{minimize}} \quad & \sum_{t=1}^{T} u_t^\intercal P_t u_t \\ \text{subject to} \quad & (B_{\text{Pursuer}} \otimes I_n) u_t = p_t - p_{t-1} \\ & u_t \in \mathcal{U}^n \end{aligned} \tag{P2}$$

for positive semi-definite matrices $P_t \in \mathbb{R}^{2n\times 2n}$, and B_{Pursuer} as defined in (4). This optimization problem generates a sequence of control actions that minimizes the control effort to drive the pursuer from the initial position to the desired location.

IV. Experimental Results

We evaluate our method on a variety of scenarios, designed to validate our approach and elucidate relevant phenomena. In all scenarios, we consider an environment with $Q = [-2, 2] \times [-2, 2] \subseteq \mathbb{R}^2$ and a time horizon of length $T = 30$. All numerical computations were implemented in MATLAB R2018a on an Intel Core i7 CPU with 3.6GHz clock rate and 16GB RAM. We employed MATLAB's nonlinear solver, *fmincon*, to implement an SQP-based solution to (P1), and CVX to implement the solution to (P2. All optimizations of (P1) were implemented in a one-step horizon as in [8], in an iterative fashion over 30 time steps.

We presume 2D point-mass pursuer dynamics, with $A_{\text{Pursuer}} = I_2$, and $B_{\text{Pursuer}} = T_s I_2$, input bounds $\mathcal{U} = [-1, 1] \times [-1, 1]$ and sampling time $T_s = 0.1$. The sensing

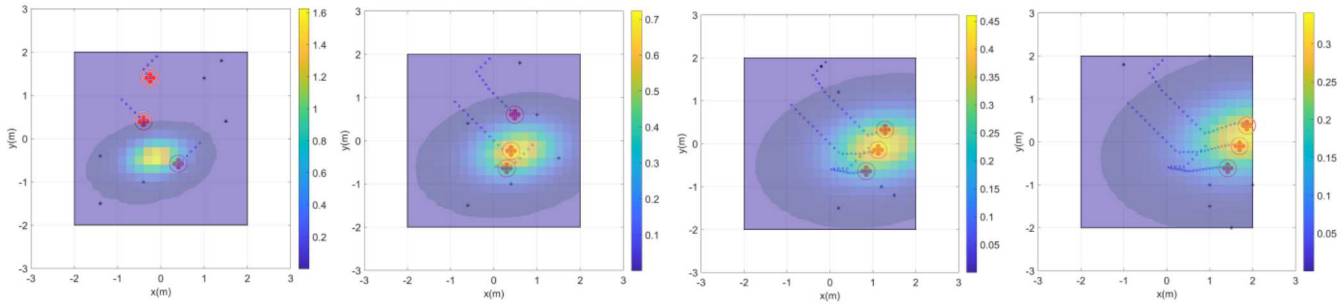

Fig. 4. Snapshots of target mean position (black '*') and pursuer trajectories (green, blue, and red squares) at $t = 6$, $t = 14$, $t = 22$, and $t = 30$, respectively (left to right). The initial conditions for the pursuers are $p_0^1 = [0\ \ 2]^\intercal$, $p_0^2 = [-1\ \ 1]^\intercal$, $p_0^3 = [1\ \ 0]^\intercal$, and the initial conditions for targets are $x_0^1 = [-2\ \ -1]^\intercal$, $x_0^2 = [-1\ \ -1]^\intercal$, $x_0^3 = [-2\ \ -1.5]^\intercal$, $x_0^4 = [1\ 2]^\intercal$,$x_0^5 = [2\ 1.8]^\intercal$, $x_0^6 = [1.5\ 1]^\intercal$.

Target No.	Mean	Covariance
1	$\mu_0^1 = \begin{bmatrix} 1 & 1 \end{bmatrix}^\intercal$	$\Sigma_0^1 = \begin{bmatrix} 2.5 & 0.3 \\ 0.3 & 1 \end{bmatrix}$
2	$\mu_0^2 = \begin{bmatrix} 1 & 0 \end{bmatrix}^\intercal$	$\Sigma_0^2 = \begin{bmatrix} 2 & 3 \\ 3 & 6 \end{bmatrix}$
3	$\mu_0^3 = \mu_0^2$	$\Sigma_0^3 = \begin{bmatrix} 0.5 & 0.75 \\ 0.75 & 1.5 \end{bmatrix}$
4	$\mu_0^4 = \begin{bmatrix} 0 & -1 \end{bmatrix}^\intercal$	$\Sigma_0^4 = \begin{bmatrix} 3 & 4.5 \\ 4.5 & 9 \end{bmatrix}$
5	$\mu_0^5 = \begin{bmatrix} -1 & 0 \end{bmatrix}^\intercal$	$\Sigma_0^5 = \begin{bmatrix} 4 & 6 \\ 6 & 3 \end{bmatrix}$
6	$\mu_0^6 = \mu_0^4$	$\Sigma_0^6 = \begin{bmatrix} 1 & 1.5 \\ 1.5 & 3 \end{bmatrix}$
7	$\mu_0^7 = \mu_0^6$	$\Sigma_0^7 = \Sigma_0^6$
8	$\mu_0^8 = \begin{bmatrix} -1 & 1 \end{bmatrix}^\intercal$	$\Sigma_0^8 = \Sigma_0^7$
9	$\mu_0^9 = \mu_0^2$	$\Sigma_0^9 = \Sigma_0^8$
10	$\mu_0^{10} = \mu_0^9$	$\Sigma_0^{10} = \Sigma_0^9$

TABLE I

TARGET STOCHASTICITY, $\mathcal{N}(\mu, \Sigma)$, FOR UP TO 10 TARGETS

function (6) has constants $\lambda_i = 0.25$, $f^{i0} = 1$ for $i \in \{1, \ldots, n\}$, meaning that all pursuers are similarly equipped. We presume that the safety radius is $r_{\min} = 0.2$.

The target dynamics are described by

$$x_{t+1}^i = x_t^i + B\omega_t^i, \tag{18}$$

$$\omega_t^i \sim \mathcal{N}(\mu^i, \Sigma^i) \tag{19}$$

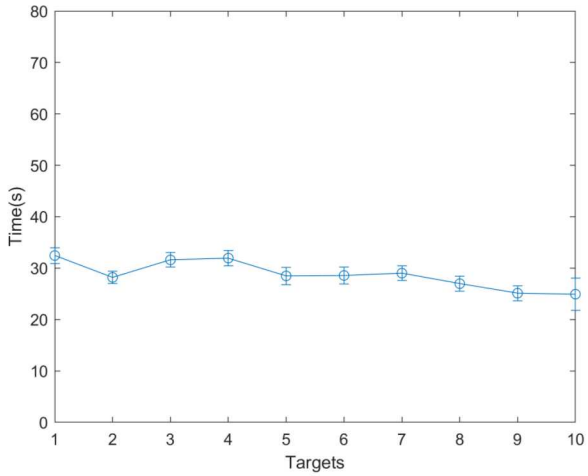

Fig. 5. Computation time with varying number of targets for $n = 5$ pursuers, based on 20 simulations for each scenario (from the same initial condition).

with $B = B_{\text{Pursuer}}$.

We consider scenarios with up to 10 targets, for which we specify a variety of means and variances (Table I).

Fig. 4 depicts a representative scenario with more targets than pursuers. As expected, the pursuers move towards areas of high likelihood of target detection, while maintaining separation mandated by collision avoidance. The sensor performance function decays relatively slowly, so the relative merit of joint sensing, rather than the collision avoidance radius, is the predominant factor in determining spacing between pursuers. For this scenario, computation time was 25.1 seconds.

We fixed the number of pursuers at $n = 5$, and ran 20 simulations from the same initial condition for varying numbers of targets. The mean and standard deviations in computation time are shown in Fig. 5. As expected, the computation time is independent of the number of targets.

We then fixed the number of targets at 5 and varied the number of pursuers from $n = 1$ to $n = 10$, again running 20

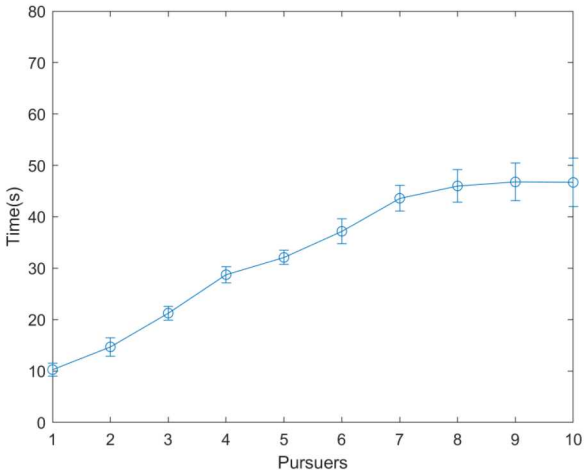

Fig. 6. Computation time with varying number of pursuers for five targets, based on 20 simulations for each scenario (from the same initial condition).

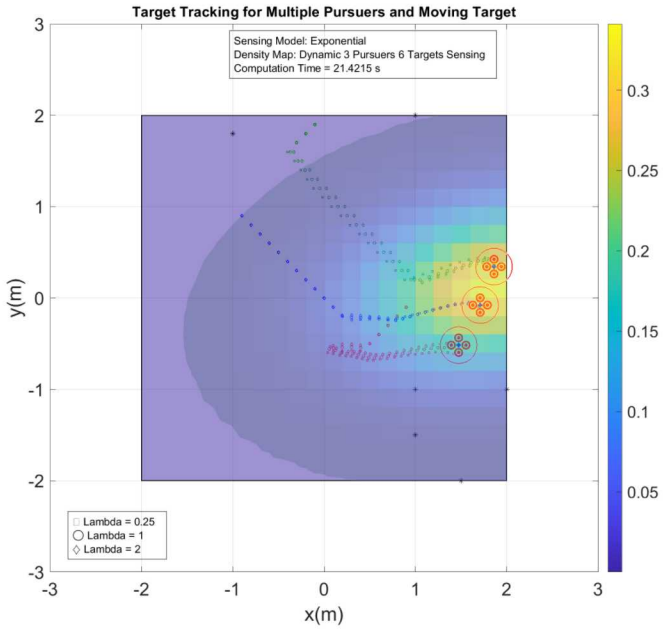

Fig. 7. Snapshot of the final configuration (at $t = 30$) for the 3 pursuer, 6 target scenario. The black '*' indicate the targets' final expected position. Trajectories for pursuer 1, pursuer 2, and pursuer 3 are indicated by green, blue, and red, respectively. The squares, circles, and diamonds, depict the pursuers' trajectories under three different sensing functions, determined by $\lambda_i = 0.25$, $\lambda_i = 1$, and $\lambda_i = 2$, respectively, for $i \in \{1, \ldots, n\}$.

simulations from the same initial condition. The mean and standard deviations for computation time are shown in Figure 6. As expected, the computational time increases as the number of pursuers increases, due to the additional decision variables. However, for higher numbers of pursuers, there is not much corresponding increase in computation time. This is ostensibly due to the fact that the space is "saturated" with pursuers, and the increased coverage from the additional pursuers is essentially trivial.

For a scenario in which there are 6 targets and 3 pursuers, we evaluated the effect of the sensing function decay rate. For a given disturbance sequence and a fixed initial condition, we simulated trajectories for $\lambda_i = 0.25$, $\lambda_i = 1$, $\lambda_i = 2$ (i.e., all three sensing functions depicted in Figure 2). As before, we presume that the decay constant is the same for all pursuers. As shown in Figure 7, the trajectories are fairly similar, with slightly more spread amongst the pursuers for lower decay rates. Because each UAV can assure high quality information over a broader region in this case, the UAVs can spread out to capture more of the underlying distribution.

We computed the corresponding optimal control for this scenario by solving (P2) with $P_t = I_{2n}$ (i.e., minimizing control effort) for each of the three values of λ_i. We computed the 2-norm of the control effort for each pursuer. In Figure 8, we see that the total control effort is shared amongst pursuers due to the coupling inherent in the joint likelihood of detection (13), and that as expected, the control effort does not vary excessively for different sensing function decay rates.

V. Conclusion

We presented a solution for simultaneous coverage and tracking of multiple targets with stochastic dynamics in by multiple pursuers. We constructed a variant of an expected value multi-center function, to capture the expected likelihood of target locations, weighted by sensing limitations of the pursuers. By maximizing this function, subject to one-step reachability constraints to capture the pursuer dynamics, we obtain feasible pursuer trajectories that accommodate joint sensing in a dynamic, stochastic environment. We implemented our approach using sequential quadratic program to solve for the local optima of the resulting nonlinear constrained optimization problem. We constructed an optimal open-loop control sequence from the optimized pursuer trajectories, to drive the pursuers to the desired locations. Numerical examples were shown to validate the proposed algorithm.

References

[1] J. Cortes, S. Martinez, and F. Bullo, "Spatially-distributed coverage optimization and control with limited-range interactions," *ESAIM: Control, Optimisation and Calculus of Variations*, vol. 11, no. 4, pp. 691–719, 2005.

[2] L. C. A. Pimenta, V. Kumar, R. C. Mesquita, and G. A. S. Pereira, "Sensing and coverage for a network of heterogeneous robots," in *Proceedings of the IEEE Conference on Decision and Control*, Dec 2008, pp. 3947–3952.

[3] F. Bullo, J. Cortes, and S. Martinez, *Distributed control of robotic networks: A mathematical approach to motion coordination algorithms*. Princeton University Press, 2009, vol. 27.

[4] S. G. Lee, Y. Diaz-Mercado, and M. Egerstedt, "Multirobot control using time-varying density functions," *IEEE Transactions on Robotics*, vol. 31, no. 2, pp. 489–493, April 2015.

[5] L. C. Pimenta, M. Schwager, Q. Lindsey, V. Kumar, D. Rus, R. C. Mesquita, and G. A. Pereira, "Simultaneous coverage and tracking (scat) of moving targets with robot networks," in *Algorithmic Foundation of Robotics VIII*, 2009, pp. 85–99.

[6] S. Miah, A. Y. Panah, M. M. H. Fallah, and D. Spinello, "Generalized non-autonomous metric optimization for area coverage problems with mobile autonomous agents," *Automatica*, vol. 80, pp. 295–299, 2017.

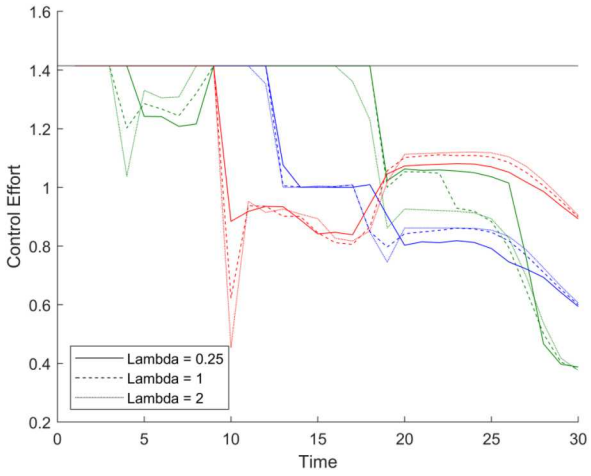

Fig. 8. Control effort for the 3 pursuer, 6 target scenario, corresponding to the trajectories shown in Fig. 7, for $\lambda = 0.25$, $\lambda = 1$, and $\lambda = 2$, respectively. The green, blue and red, indicated the control effort for pursuer 1, pursuer 2 and pursuer 3, respectively.

[7] M. Schwager, D. Rus, and J.-J. Slotine, "Decentralized, adaptive coverage control for networked robots," *The International Journal of Robotics Research*, vol. 28, no. 3, pp. 357–375, 2009.

[8] G. M. Hoffmann and C. J. Tomlin, "Mobile sensor network control using mutual information methods and particle filters," *IEEE Transactions on Automatic Control*, vol. 55, no. 1, pp. 32–47, Jan 2010.

[9] B. J. Julian, M. Angermann, M. Schwager, and D. Rus, "Distributed robotic sensor networks: An information-theoretic approach," *The International Journal of Robotics Research*, vol. 31, no. 10, pp. 1134–1154, 2012.

[10] P. Dames and V. Kumar, "Autonomous localization of an unknown number of targets without data association using teams of mobile sensors," *IEEE Transactions on Automation Science and Engineering*, vol. 12, no. 3, pp. 850–864, July 2015.

[11] A. Mavrommati, E. Tzorakoleftherakis, I. Abraham, and T. D. Murphey, "Real-time area coverage and target localization using receding-horizon ergodic exploration," *IEEE Transactions on Robotics*, vol. 34, no. 1, pp. 62–80, Feb 2018.

[12] I. Abraham and T. D. Murphey, "Decentralized ergodic control: Distribution-driven sensing and exploration for multiagent systems," *IEEE Robotics and Automation Letters*, vol. 3, no. 4, pp. 2987–2994, Oct 2018.

[13] M. Zhong and C. G. Cassandras, "Distributed coverage control and data collection with mobile sensor networks," *IEEE Transactions on Automatic Control*, vol. 56, no. 10, pp. 2445–2455, 2011.

[14] N. Zhou, C. G. Cassandras, X. Yu, and S. B. Andersson, "Decentralized event-driven algorithms for multi-agent persistent monitoring tasks," in *Proceedings of the IEEE Conference on Decision and Control*, Dec 2017, pp. 4064–4069.

[15] T. Clouqueur, V. Phipatanasuphorn, P. Ramanathan, and K. K. Saluja, "Sensor deployment strategy for target detection," in *Proceedings of the 1st ACM international workshop on Wireless sensor networks and applications*. ACM, 2002, pp. 42–48.

[16] S. S. Iyengar and R. R. Brooks, *Distributed Sensor Networks: Sensor Networking and Applications (Volume Two)*. CRC press, 2016.

[17] A. P. Vinod, B. HomChaudhuri, and M. M. Oishi, "Forward stochastic reachability analysis for uncontrolled linear systems using fourier transforms," in *Proceedings of the International Conference on Hybrid Systems: Computation and Control*. ACM, 2017, pp. 35–44.

[18] P. Billingsley, *Probability and measure*. John Wiley & Sons, 2008.

[19] M. Khaledyan, A. P. Vinod, M. Oishi, and J. A. Richards, "Optimal coverage control and stochastic multi-target tracking," in *IEEE Conference on Decision and Control*. IEEE, 2019, pp. 2473–2478.

[20] F. Blanchini and S. Miani, *Set-theoretic methods in control*. Springer, 2008.

[21] M. Herceg, M. Kvasnica, C. N. Jones, and M. Morari, "Multi-parametric toolbox 3.0," in *Proceedings of IEEE European Control Conference*, 2013, pp. 502–510.

[22] J. Nocedal and S. Wright, *Numerical optimization*. Springer Science & Business Media, 2006.

[23] R. H. Byrd, M. E. Hribar, and J. Nocedal, "An interior point algorithm for large-scale nonlinear programming," *SIAM Journal on Optimization*, vol. 9, no. 4, pp. 877–900, 1999.

[24] T. Lipp and S. Boyd, "Variations and extension of the convex-concave procedure," vol. 17, 2016, pp. 263–287.

[25] J. L. Williams, "Information theoretic sensor management," Ph.D. dissertation, Massachusetts Institute of Technology, 2007.